A mathematical model of the nicotinic-agonist stimulated release of dopamine from striatal synaptosomes

M. S. Penney[1], N. F. Britton[1], L. Soliakov[2] and S. Wonnacott[2]
Department of Mathematical Sciences[1] and Department of Biology and Biochemistry[2], University of Bath, Bath, BA2 7AY, UK.
E-mail: M.S.Penney@bath.ac.uk

March, 1999

Abstract

The elicitation of dopamine release from rat striatal synaptosomes by KCl stimulation and nicotinic agonists has been well characterised experimentally. Based on these data we have produced a mathematical model of the population of striatal dopaminergic nerve terminals. This model predicts that KCl evokes release by causing a single clamped membrane depolarisation that is independent of the involvement of voltage-sensitive Na^+ channels, whereas nicotinic agonists produce a series of Na^+ channel induced action potentials that is only attenuated by receptor desensitisation or agonist removal and such release is limited only by the availability of readily-releasable transmitter and its rate of replacement. Analysis of these modes of inducing transmitter release allows us to estimate the existence of three major sub-populations of dopamine terminal.

1 Introduction

Neurotransmitter release is not only influenced by the arrival of an action potential at the nerve terminal, it is subject to both positive and negative modulation by a variety of presynaptic receptors [13]. The stimulation of transmitter release by presynaptic nicotinic acetylcholine receptors (nAChR) in the brain has been widely documented and is considered to constitute a significant physiological role of these ligand gated ion channels [22] [30]. The nicotinic stimulation of dopamine release from striatal synaptosomes has been the subject of detailed examination [4] [6] [20] [21]. More recently we have explored the mechanism of this nicotinic modulation, using anatoxin-a (AnTx) as the agonist of choice, by virtue of its potency, stability and specificity [25] [26].

These data have been used to create a mathematical model of this experimental preparation. We have done this by first producing models of individual nerve terminals. Each terminal is considered to be a single electrical compartment with Hodgkin and Huxley models of voltage-sensitive potassium, sodium and calcium channels. The proportions of different calcium channels and nAChR varies between terminals, giving rise to a number of sub-populations. The model is therefore a system of nonlinear ordinary differential equations which can be solved numerically. Transmitter release is then calculated from the calcium influx. Optimising the fit of the results for the experimental preparation dictates the proportions of the sub-populations. This approach enables us to fit, reproduce and then predict the results of a range of synaptosome experiments, as well as providing a subcellular view and subsecond time resolution of nerve terminal events. Hence not only can we match the experimental set up, we can also produce sound hypotheses of individual nerve terminal function from observations of large populations.

2 Methods

2.1 Experimental Background

The modelling is based largely on the results of synaptosome experiments [25] [26] and it is pertinent to briefly summarise the salient features here. Synaptosomes were prepared from rat striata, loaded with [^{3}H]dopamine, placed in superfusion chambers and superfused with a standard Krebs Ringer buffer, supplemented with ascorbic acid, pargyline and (after loading) nomifensine. Once a stable baseline was obtained, a 40s pulse of KCl or AnTx was delivered; 2 min fractions were collected to estimate the amount of release. Antagonists and other drugs were introduced 10 min prior to agonist / KCl and maintained throughout.

2.2 The Basic Terminal

We regard a synaptosome to be a single compartment 1 micron in diameter and length. Since this compartment is physiologically small we consider it to be isopotential, that is the membrane potential is the voltage potential of the whole cell and hence there are no effects from the spatial distribution of ion channels or receptors. The compartment has a specific membrane resistance R_M and capacitance C_M which are those values used by Traub et al [27] in their model of rat hippocampal neurons, adjusted for cell size.

Four types of voltage-activated ion channels are included in the model, two selective for calcium and one each for potassium or sodium. The ion flux (I) through a set of channels is regarded as an electrical current and hence obeys Ohm's Law

$$I = g(E - V_m) \tag{1}$$

where g is the conductance of the channels (a function of total number of channels, channel activation and inactivation due to voltage and time). $(E - V_m)$ is the difference between the membrane potential V_m and the reversal potential of the ion species E and represents the voltage gradient across the membrane.

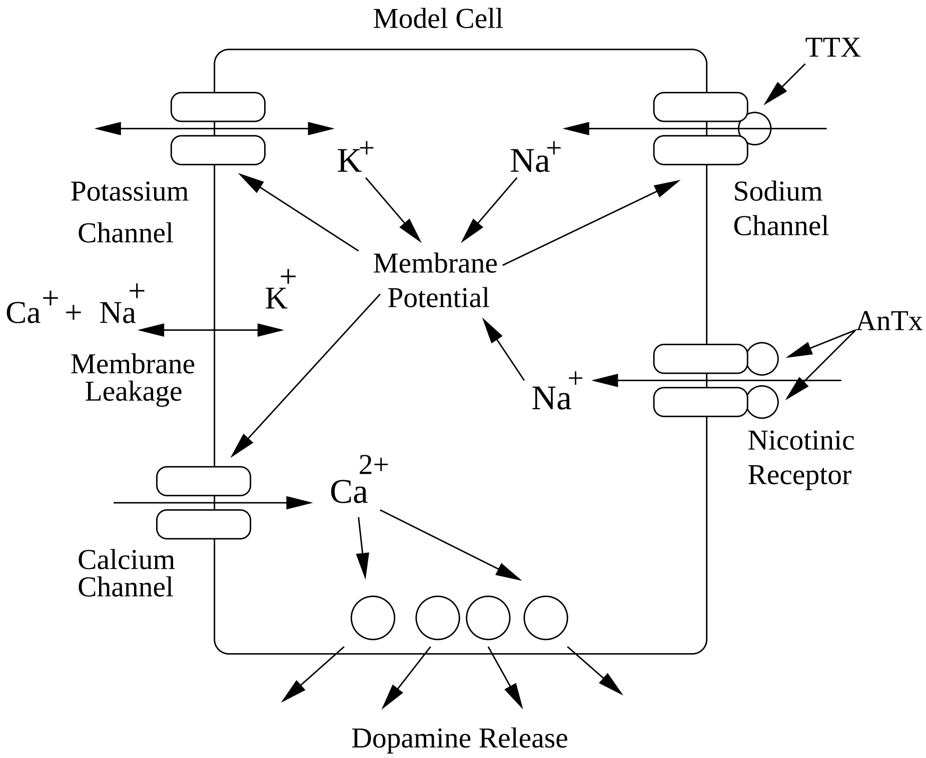

Figure 1: Schematic diagram of the model cell showing the interactions between the components.

2.2.1 Calcium Ion Channels

We implement models of N-type and P-type voltage-activated calcium channels, it having been shown that KCl-evoked release of [^{3}H]dopamine from striatal synaptosomes is blocked by the selective antagonists of N- and P-types, $\omega-$Conotoxin GVIA (ω-CgTx) and $\omega-$Agatoxin IVA (ω-Aga IVA) respectively [26]. It is not completely clear from this whether N- and P-types coexist on terminals (and by some mechanism AnTx only causes the activation of N-types) or terminals possess one type exclusively. We use the latter, simpler, hypothesis that a terminal may contain either N- or P-type channels, but not both.

Voltage-dependent activation $x_\infty(V_m)$ and inactivation $y_\infty(V_m)$ curves for N-type channels were taken from McNaughton et al [15]. The time dependence of activation τ_x is taken from [19] and the inactivation τ_y then chosen to be consistent with the experimental data [15]. The P-type calcium channel voltage-dependent activation curve $p_\infty(V_m)$ is taken from [29] and time constant of activation τ_p from [19]. The currents are given by:

$$\begin{aligned}
I_{\mathrm{N}} &= \bar{g_{\mathrm{N}}} xy(E_{\mathrm{Ca}} - V_m) \\
\frac{dx}{dt} &= \frac{x_\infty(V_m) - x}{\tau_x} \\
\frac{dy}{dt} &= \frac{y_\infty(V_m) - y}{\tau_y} \\
I_{\mathrm{P}} &= \bar{g_{\mathrm{P}}} p(E_{\mathrm{Ca}} - V_m)
\end{aligned}$$

$$\frac{dp}{dt} = \frac{p_\infty(V_m) - p}{\tau_p}$$

with the details given in appendices B.5 and B.6. The conductances $\bar{g_{\rm N}}$ and $\bar{g_{\rm P}}$ may be calculated from known conductance densities for cell size [24]. This gives total conductances of the order of 10^{-10}Siemens, which implies that the calcium currents are negligible compared to the other currents used. Hence both channels are excluded in the computation of the membrane potential, although we use this calcium influx to calculate the amount of transmitter release.

2.2.2 Potassium Ion Channels

We include a delayed-rectifying potassium channel. The voltage dependent kinetics $\alpha(V_m)$ and $\beta(V_m)$ are taken from electrophysiological measurements on the rat hippocampus [23]. The conductance $\bar{g_{\rm K}}$ (in combination with the leakage reversal potential, see section 2.2.4) is set so that the cell rests at -78mV [23]. The current is therefore given by:

$$\begin{aligned} I_{\rm K} &= \bar{g_{\rm K}} m(E_{\rm K} - V_m) \\ \frac{dm}{dt} &= \alpha_m(V_m)(1-m) - \beta_m(V_m)m \end{aligned}$$

see appendix B.3 for details.

We can model the stimulation of the experimental preparation by KCL by changing the extracellular concentration of potassium appropriately. The subsequent shift in the reversal potential $E_{\rm K}$ may cause potassium influx, depolarising the cell.

2.2.3 Sodium Ion Channels

We take fast sodium channel kinetics from the rat hippocampus as described by [23]. The channel conductance $\bar{g_{\rm Na}}$ is set so that doses of AnTx of 1μM and above produce sodium channel-induced action potentials. We model the effects of the voltage-activated sodium channel blocker tetrodotoxin (TTX) by reducing the conductance of the sodium channels to zero. The current is given by:

$$\begin{aligned} I_{\rm Na} &= \bar{g_{\rm Na}} r^2 s(E_{\rm Na} - V_m) \\ \frac{dr}{dt} &= \alpha_r(V_m)(1-r) - \beta_r(V_m)r \\ \frac{ds}{dt} &= \alpha_s(V_m)(1-s) - \beta_s(V_m)s \end{aligned}$$

see appendix B.4 for details.

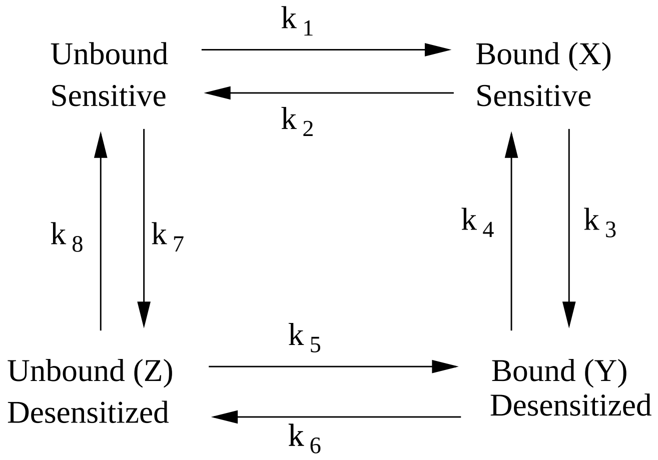

Figure 2: Receptor binding site state transition model [14]. For the receptor pore to open, both binding sites must be in the bound and sensitive state (X). The constants k_i are determined from experimentation.

2.2.4 Leakage Current

Due to the natural permeability of the cell membrane and the action of ion pumps, there will be some ion flux across it aside from the ion channels included[2]. We model this by assuming a leakage current given by

$$I_{\text{leak}} = \frac{E_m - V_m}{R_m} \tag{2}$$

where E_m is the reverse potential of this current, V_m the membrane potential and R_m the membrane electrical resistance. R_m is already fixed due to the cell dimensions and the specific resistance of [27], whereas E_m is set so that the modelled effect of the leakage and ion pumps in combination with the ion channels allows the cell to rest at -78mV [23] and are given in appendix B.7.

2.3 Nicotinic Acetylcholine Receptor

For simplicity we take the nACh receptors to be homogeneous and then take the channel opening and closing kinetics from the analysis of the binding of [^{3}H]nicotine to rat brain sites [14] where the initial, low affinity binding rate is proposed to reflect binding to the active conformation of the receptor. In this model, each receptor has two binding sites for nicotinic agonists and we assume that ligand binding to both is required for channel opening. Each binding site has four states; unbound and sensitive; bound and sensitive (permissible for pore opening); bound and desensitized; unbound and desensitized, see figure 2.3.

If we let $X, Y, Z \in [0, 1]$ be the proportion of binding sites that are bound and sensitive; bound and desensitized; and unbound and desensitized respectively; then by the above assumptions X^2 is the proportion of receptors that are gating ion flux. Hence the channel conductance g in equation (1) is given by $\bar{g_R}X^2$, where $\bar{g_R}$ is the total channel conductance, set such that concentrations of 1μM AnTx or above produce an action potential in the model cell. From [14] the binding site state transition equations are:

$$\frac{dX}{dt} = k_1[\mathrm{n}](1 - X - Y - Z) + k_4Y - k_2X - k_3X \tag{3}$$

$$\frac{dY}{dt} = k_3X - k_4Y + k_5[\mathrm{n}]Z - k_6Y \tag{4}$$

$$\frac{dZ}{dt} = k_7(1 - X - Y - Z) - k_8Z + k_6Y - k_5[\mathrm{n}]Z \tag{5}$$

where [n] is agonist concentration and the k_is are experimentally derived constants [14] as given in appendix B.8.

2.4 Transmitter Release

We include two components of release; one is a simple model to reflect the calcium-dependent release from a cell with constant membrane potential, while the other is more complex designed to model release caused by depolarisation of the membrane. The equations and parameters are detailed in appendix B.9.

2.4.1 Internal Calcium Concentration due to an Open Channel

By the calcium hypothesis of transmitter release calcium [3] influx through a calcium channel can cause vesicle exocytosis by interacting with binding sites close to the cytoplasmic end of the channel. We therefore take the probability of influx causing release to be a function of the concentration of calcium close to the end of the channel.

In the model, calcium flows in under a voltage gradient given by $(E_{\mathrm{Ca}} - V_m)$, where $E_{\mathrm{Ca}} = \frac{RT}{F\mathrm{v}} \ln\left(\frac{[\mathrm{Ca}]_\mathrm{o}}{[\mathrm{Ca}]_\mathrm{i}}\right)$ is the reversal potential for calcium, V_m is the membrane potential, R the universal gas constant, T the temperature in Kelvin, F Faraday's constant and v the valency of the ion. Influx will continue until this gradient is reduced to zero. As the terminal is isopotential and hence there are no local changes in voltage,the membrane potential will not change. Instead the internal calcium concentration local to the channel end will rise until

$$[\mathrm{Ca}]_\mathrm{i} = c([\mathrm{Ca}]_\mathrm{o}, V_m) := [\mathrm{Ca}]_\mathrm{o} \exp\left(-\frac{V_m F\mathrm{v}}{RT}\right) \tag{6}$$

where $[\mathrm{Ca}]_\mathrm{o}$ is the extracellular concentration of calcium.

2.4.2 Transmitter Release due to Change of Membrane Potential

Superfusion experimental set-ups with subsecond resolution demonstrate that the majority of KCl-induced transmitter release occurs directly after the application of the stimulation [28]. This suggests that it is a step in membrane potential causing the large amount of release and so we make the following assumptions on our model:

One; the change in membrane potential causes the simultaneous opening of many channels around vesicle release sites, thus providing sufficient influx to cause significantly large amounts of transmitter release.

Two; there is a delay between the change in potential and the opening of the channels. We take this to be the average time to open for a single channel. For a channel modelled using the formulation of Hodgkin and Huxley [8] with time constant of activation τ, the average time to open is $\ln(2)\tau$. This gives times to open for N- and P-type channels of about 0.7ms and 0.8ms respectively. Such times are consistent with observed delays between membrane depolarisation and calcium influx [1].

As a consequence to this, should the depolarising influence behind a channel opening be removed before the channel has opened, then the channel does not open. Hence the depolarisation must last for the period of the time lag.

The motivation for including this lag is the experimental result that the application of the voltage-activated sodium channel antagonist TTX does not affect release evoked by 20mM KCl[25]. It has been hypothesised that this is because the action potential depolarisation is over too quickly to open (significantly) more calcium channels than will be opened by the KCl depolarisation without action potential (KCl dose with TTX). Hence the only part of the action potential depolarisation that is effective in terms of transmitter release is that which is maintained for the prescribed time lag.

Three; channel inactivation is negligible for N-type calcium channels since we depolarise from largely negative potentials where inactivation is small and take the rate of depolarisation to be fast in comparison to channel inactivation rate.

Four; there is a finite pool of transmitter available for release. This pool is replenished at a constant rate, however this rate is slow in the sense that repetitive firing of action potentials cannot be supported for more than a few seconds. This is consistent with experimental observations [5] [25] and may be explained by the use of nomifensine in the superfusion experiments to disable the reuptake and recycling of transmitter by transporter, slowing pool replenishment.

Five; we assume that release is proportional to the number of opened channels multiplied by (some power of) the internal calcium concentration achieved, provided of course that sufficient transmitter is available. As the change in open channels for a change in voltage is $\frac{d}{dV}x_\infty(V)$, for channel activation curve $x_\infty(V)$, we have the expected release rate $\frac{dR}{dt}(t)$ from a terminal with channels of time lag T to be:

$$\frac{dR}{dt}(t) = \begin{cases} 0 & \text{if } V(t-T) > \inf\{V(\tau) : t-T < \tau < t\}, \\ K\frac{d}{dV}x_\infty(V(t-T))c([\mathrm{Ca}]_o, V(t))^n & \text{otherwise} \end{cases} \tag{7}$$

where K is a constant to be determined by fitting the model to the experimental data and n is the dependency of release on internal calcium concentration. Note that the index to the number of channels opened is evaluated at time $(t-T)$, although the current would then flow under the voltage gradient at time t.

2.4.3 Steady-state Transmitter Release

We present a simple model of this form of release and assume that is proportional to the number of (hence proportion of) open channels multiplied by (some power of) the internal calcium concentration achieved due to an open channel. Hence for calcium influx through

N-type channels

$$\text{Release per second} = K_N x_\infty(V_m) y_\infty(V_m) c([\mathrm{Ca}]_o, V_m)^2 \tag{8}$$

where K_N is a constant to be determined, x_∞ and y_∞ are the voltage dependent activation and inactivation curves for N-type channels and $c([\mathrm{Ca}]_o, V)$ is the internal calcium concentration as described above. Similarly for P-type channels

$$\text{Release per second} = K_P p_\infty(V_m) c([\mathrm{Ca}]_o, V_m)^4 \tag{9}$$

where K_P is a constant to be determined by fitting to experimental data and p_∞ is the voltage dependent activation of P-type channels (which have no voltage dependent inactivation). The use of the second power of calcium concentration for N-type channels and the fourth power for P-types comes from the model of release for changes in membrane potential below.

3 Results

The complexity of the model, a system of thirteen nonlinear ordinary differential equations, means that we have not searched for an analytical solution. However, the qualitative features of the model solutions are quite simple. In the absence of simulated KCl or nicotinic stimulation, the model rests at a steady voltage of -78mV. Stimulation by raising KCl levels produces a shift in the steady state to a more depolarised value and hence there is a transient rise in membrane potential before the cell rests at this new voltage. For sufficiently large concentrations of KCl, and in the absence of any blocking of the sodium channels, this transient may feature a large deviation, that is an action potential, before resting.

Nicotinic stimulation also causes a shift in the steady state voltage of the system and numerical results suggest that sufficiently high concentrations of AnTx cause the model to transiently fire repetitive action potentials via a Hopf bifurcation. For the calculation of transmitter release and fitting to the experimental data, the model was implemented on the neural simulator GENESIS [2] and solved numerically using the exponential Euler method, which is optimal for the solution of equations such as equation (10).

The experimental data ([5][25][26] and Table 1) can be summarised as follows: KCl causes a dose-dependent release of dopamine up to a maximum at 50mM KCl; the nicotinic agonist AnTx also causes a dose-dependent release but the maximum response is only 20% of that achieved by KCl[25]. While KCl-elicited release is blocked equally and additively by the N- and P-type calcium channel blockers ω-conotoxin GVIA (ω-CgTx) and ω-agatoxin IVA (ω-Aga IVA) respectively, AnTx-elicited release is predominantly blocked by ω-CgTx and insensitive to ω-Aga IVA [26]. The sodium channel blocker tetrodotoxin (TTX) does not affect release elicited by 20mM KCl [25]: KCl depolarises the terminals by shifting the potassium reversal potential, causing an inward current. This will cause the transient opening of sodium channels (in the absence of TTX) and then the cell rests close to the new reversal potential. In contrast TTX partially inhibits 1μM AnTx-evoked release [25], whereas removal of extracellular sodium increases release evoked by 25mM KCl but abolishes that evoked by 1μM AnTx, indicating that sodium channels mediate

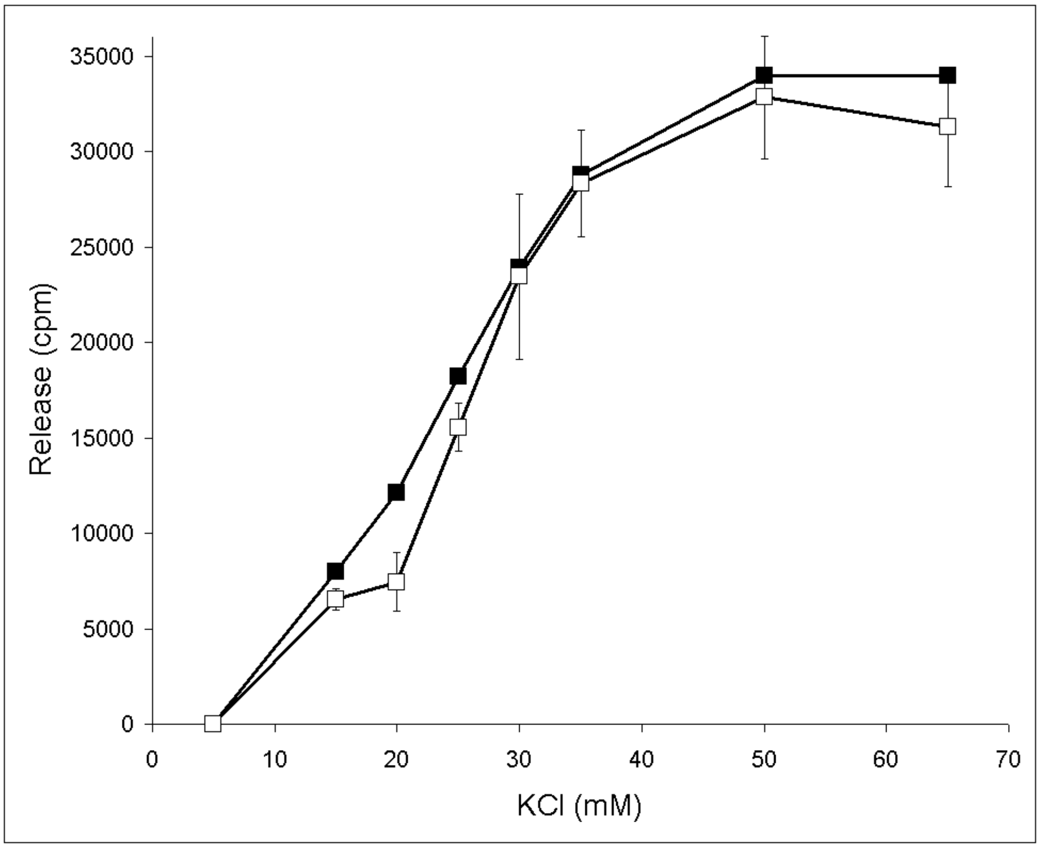

Figure 3: Comparison of dose-dependent KCl-evoked release of [^{3}H]dopamine from striatal synaptosomes, described by Soliakov et al [25] (□) and that predicted by the model (■).

some of the response [25]. There is a lack of additivity of release when sub-maximal concentrations of KCl and AnTx are applied together [25].

Based on these observations we have assumed three sub-populations of terminals: those terminals with only P-type calcium channels; terminals with only N-type calcium channels and terminals with N-type calcium channels only and nAChR. Equal proportions of terminals possessing N- and P-type calcium channels is consistent with the approximately equal and additive inhibition of KCl-evoked transmitter release by ω-CgTx and ω-Aga IVA. As AnTx-evoked release appears to be mediated by N-type calcium channels it is assumed that some sub-population of these have nAChR and for simplicity that each such terminal has the same number of functional nAChR. The proportion of such terminals in the population can then be derived from fitting the model to the AnTx-evoked release [25].

Fitting this model to the KCl-evoked release describes the data well (Fig. 3). To enforce the upper limit of KCl-evoked release, a finite supply of readily-releasable [^{3}H]dopamine with slow (order of minutes) replenishment from a reserve pool of [^{3}H]dopamine is assumed. The best fit of the model to the KCl-evoked release curve requires the assumption that release from terminals with P-type calcium channels is proportional to the fourth power of extracellular calcium, while from terminals with N-type calcium channels it is proportional to the second power.

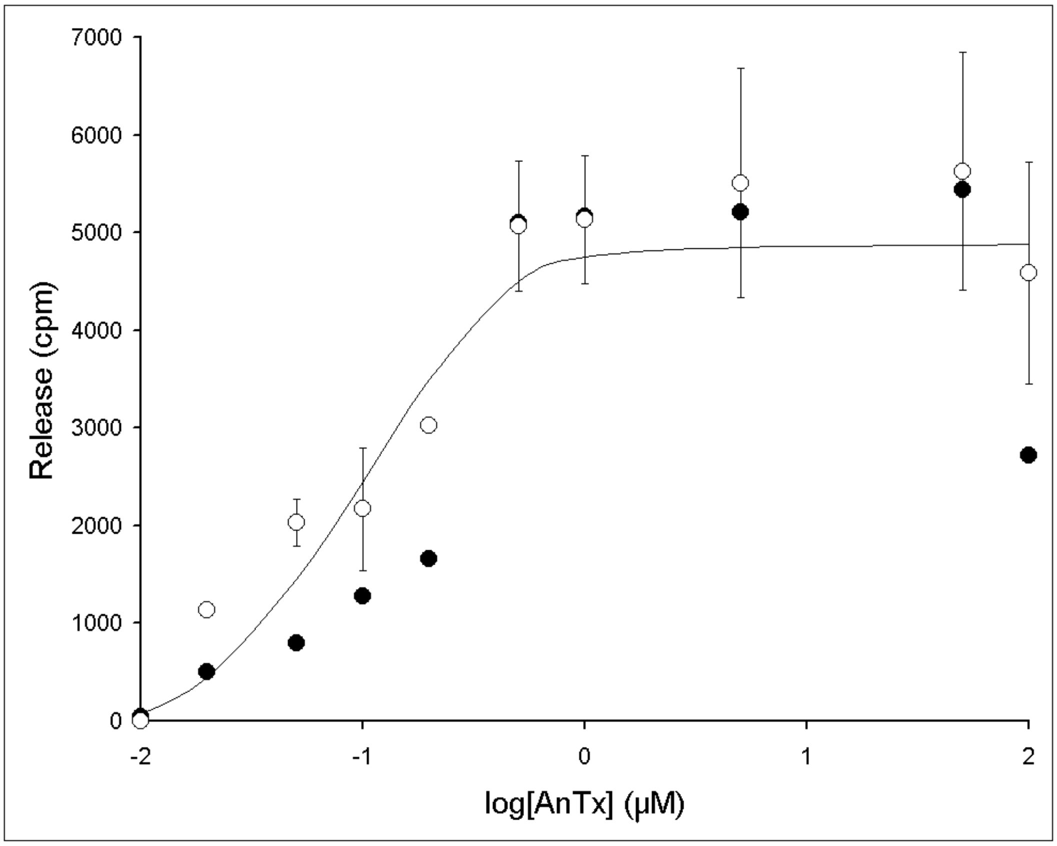

Figure 4: Comparison of dose-dependent AnTx-evoked release of [^{3}H] dopamine from striatal synaptosomes, described by Soliakov et al [25] (○) and that predicted by the model (●).

Condition	[^{3}H]dopamine release (cpm)	
	Theoretical	Experimental Data from [25]
Control 25mM KCl	18214	15558 ± 1247
25mM KCl + Low Na (10mM)	16281	25780 ± 607
25mM KCl + Ca-free	0	856 ± 31
Control 20mM KCl	11532	7449 ± 1534
20mM KCl+1.5μM TTX	10398	7821 ± 156

Table 1: The effects of different buffer conditions on [^{3}H]dopamine release evoked by KCl, comparison between the experimental results [25] and those predicted by the model.

The model for transmitter release takes into account the average time taken for the calcium channels to open (0.8ms for P-type, 0.7ms for N-type [19]). This lag means that the rising part of a sodium spike is too fast to have a significant effect on transmitter release, thus KCl-evoked release is largely independent of TTX, in agreement with experimental observations. Release evoked by 25mM KCl in the presence of low extracellular sodium shows a slight decrease in the model rather than the large increase observed experimentally, see Table 1.

Having calibrated the model to KCl-evoked release, we then examined the model with respect to AnTx-evoked release. The model predicts AnTx-evoked release that agrees well with the experimental data, see Fig. 4, with a best fit achieved for 8% of the synaptosome population having both N-type calcium channels and nAChR. The only discrepancy is a consistent underestimation of release at lower concentrations of AnTx (Fig. 4) and in the presence of TTX (Table 2). The model accurately replicates the lack of additivity of release elicited by coapplication of KCl and AnTx, see Table 2. It also proposes that sufficiently large doses of AnTx (about 1μM and above) would cause repetitive firing, release then being dependent on the availability of transmitter. Repetitive firing would be prevented in the presence of a sufficiently large concentration of KCl as the clamped depolarisation produced by the KCl will cause the persistent inactivation of sodium channels.

Condition	[^{3}H]dopamine release (cpm)	
	Theoretical	Experimental Data from [25]
Control 1μM AnTx	5165	5134 ± 654
1μM AnTx + 1.5μM TTX	1881	4213 ± 490
1μM AnTx + Low Na (10mM)	680	523 ± 93
1μM AnTx + Ca^{2+}-free	0	444 ± 199
Control 15mM KCl	8080	6536 ± 568
15mM KCl + 1μM AnTx	8176	9273 ± 2068

Table 2: The effects of differing buffer conditions on [^{3}H]dopamine release evoked by AnTx, comparison between the model and experimental results.

4 Discussion

We have derived a model that accurately represents the behaviour of rat striatal synaptosomes with respect to the evoked release of [^{3}H]dopamine in superfusion experiments [5] [25] [26]. It presents hypotheses for the mechanisms of AnTx- and KCl-evoked transmitter release and allows us to estimate the abundance of terminals possessing nAChR in the synaptosome preparation.

The model has only one qualitative fault, namely that it predicts little change in release for a concentration of 25mM KCl under conditions of low extracellular NaCl, whereas experimentally a large increase was observed [25]. Experimentally NaCl was replaced by N-methyl-D-glucamine (NMDG) to conserve the osmolarity, whereas the model only takes account of changes in the principal ions. NMDG has been shown to render the resting membrane potential of synaptosomes more negative [7], in which case depolarisation close to the potassium reversal potential (achieved by the application of 25mM KCl) would be expected to open more calcium channels than at the normal resting potential and hence cause more transmitter release.

The distinction of three major sub-types of nerve terminal is the logical conclusion from the transmitter release data for synaptosomes stimulated in conjunction with various calcium channel blockers [26]. That specific blockers for N- and P-type calcium channels block KCl-evoked release additively and equally suggests that there are distinct populations of terminals with exclusively N- or P-type channels and that there are roughly equal numbers of each. As AnTx-evoked release is significantly affected by N-type channel blockers only we deduce that nAChR only co-exist with N-type calcium channels in this preparation. The construction of the model presents a methodology to estimate the proportion of these terminals from the predictions for AnTx-evoked release, see below. We cannot exclude the possibility of some terminals having both N- and P-type calcium channels (and no nAChR), although the additivity of ω-CgTx and ω-Aga VIA in inhibiting KCl-evoked release is inconsistent with the cooperation of N- and P-type channels in mediating release and instead would require each to act independently via separate release mechanisms. We consider this an unnecessary complication.

It is often quoted that transmitter release is proportional to the fourth power of extracellular calcium [3], which fits with the description of release mediated by P-type calcium channels, but not that mediated by N-type channels (second power). Different dependencies have been determined in other preparations and it was hypothesised that these reflected the number of sites for calcium binding needed to trigger release [16]. However this aspect is not present in the model, which only considers the concentration of calcium arising from the proportion of open channels. Thus the calcium dependence seems to originate in the expression for the voltage dependence of channel activation, in the parameter that describes the steepness of transition from zero to full activation. The parameter for N-type channels is about twice that of P-type channels.

It is hard to suggest a possible biological reason for this difference in parameters given the cellular functions built into the model (we should be aware that it could be a numerical fluke). However the calcium channels are classified by their pharmacologies and it is therefore possible that the channels present in the synaptosomes may have slightly different kinetics than those used in the model. Calcium channel parameters were taken from a human N-type channel expressed in HEK293 cells and claimed to resemble a presynaptic channel [15] and P-type channels in a rat motoneuron [29]. Channel parameters from other preparations may yield different dependencies if used in the model, but we consider the channels chosen [15] [29] provide the most representative data available for nerve terminals.

It will be useful to experimentally determine the calcium dependence of release and then revise the model accordingly (this would require only a slight change in the numerical fit and would not significantly alter the results). This may be done by comparing the release evoked by 25mM KCl at two different concentrations of extracellular calcium, in the presence or absence of calcium channel antagonists. This could provide a rather interesting opportunity of being able to estimate some of the activation kinetics of presynaptic calcium channels using superfusion experiments.

To derive a value for the proportion of terminals bearing functional nAChR, it was necessary to consider not only the distribution of calcium channels but also the availability of $[^3H]$dopamine for sustained release. The repetitive firing predicted to be generated by pulses of AnTx would soon exhaust the synaptosome's pool of readily releasable $[^3H]$dopamine, hence we have estimated the rate of replenishment, based on data for mouse synaptosomes [5]. This has allowed us to estimate the release from terminals stimulated with AnTx and hence to estimate the proportion of the synaptosome population that has nAChR. A value of 8% emerges from this analysis. It was originally hypothesised [25] that the lower maximum release elicited by AnTx compared with KCl may be due to low numbers of nAChR uniformally distributed throughout the population, or sufficient receptors to have the same efficacy as KCl in releasing $[^3H]$dopamine but localised to a sub-population of terminals. The model suggests an alternative, that nAChR are restricted to a smaller proportion of terminals from which they are capable of releasing a *greater* amount of $[^3H]$dopamine than KCl acting on the same terminals. Indeed, this property would explain why, in some preparations such as adrenal chromaffin cells [17], AnTx is more efficacious in releasing neurotransmitter than KCl.

The model assumes a homogeneous population of nAChR. However, recent studies provide evidence for the heterogeneity of nAChR on dopamine synaptosomes [10][12]. The $\alpha3\beta2$ sub-type of nAChR selective antagonist α-conotoxin MII partially blocks $[^3H]$dopamine release elicited by AnTx [10] or nicotine [12], consistent with the involvement of two or more subtypes of nAChR, one of which has an $\alpha3\beta2$ interface. It is not known if different nAChR reside on the same terminals or if they are segregated to separate terminals. It is possible to extend the model to account for nAChR heterogeneity by including terminal sub-types with appropriate sub-types of nAChR. Fitting this model to the release data for a nicotinic agonist in combination with a selective antagonist of one of the sub-types, such as α-conotoxin MII, would enable us to estimate the proportions of the sub-types in the population.

The model has been based on our studies using AnTx as an agonist. The estimate of 8% of dopamine terminals having nAChR assumes that all these receptors are fully sensitive to AnTx. However, other nicotinic agonists elicit $[^3H]$dopamine release from striatal synaptosomes with varying efficacies [9]. The model can accomodate such experimental results, together with the heterogeneity of nAChR described above. For example, if one sub-type of nAChR is 50% less responsive to AnTx than to a maximally efficacious agonist, that sub-type may need to be present on a further 4% of the terminals. Hence such considerations have only small effects on the prediction of the proportion of dopamine terminals bearing nAChR. It is noteworthy that such a description requires that the sub-types are segregated to separate terminals.

In conclusion, we have produced a mathematical model of the nicotinic stimulation of $[^3H]$-dopamine release from striatal synaptosomes that not only reproduces the experimental data well, but also provides sound reasons for some of the experimental observations made, such as the lack of additivity between submaximal concentrations of KCl and AnTx, and generates testable hypotheses. This exercise in modelling a relatively simple system can be refined to take account of additional physiological parameters, to extend the model for nerve terminals in more holistic preparations such as slices.

References

[1] J. G. G. Borst and B. Sakmann. Calcium influx and transmitter release in a fast CNS synapse. *Nature*, 383:431–434, October 1996.

[2] J.M. Bower and D. Beeman. *The Book of GENESIS.* TELOS, 1995.

[3] F. A. Dodge and R. Rahamimoff. Co-operative action of calcium ions in transmitter release at the neuromuscular junction. *Journal of Physiology*, 193:419–432, 1967.

[4] H. El-Bizri and P. B. S. Clarke. Blockade of nicotinic receptor-mediated release of dopamine from striatal synaptosomes by chlorisondamine and other nicotinic antagonists administered *in vitro*. *British Journal of Pharmacology*, 111:406–413, 1994.

[5] S.R. Grady, M.J. Marks, and A.C. Collins. Desensitization of Nicotine-stimulated [^{3}H]dopamine release from mouse striatal synaptosomes. *Journal of Neurochemistry*, 62(4):848–855, 1994.

[6] S.R. Grady, M.J. Marks, S. Wonnacott, and Alan C. Collins. Characterization of nicotinic receptor-mediated [^{3}H]dopamine release from synaptosomes prepared from mouse striatum. *Journal of Neurochemistry*, 59(3), 1992.

[7] C.J. Hillard. Nicotine-induced depolarisation of cerebral cortical synaptosomes is dependent upon sodium. *Neuropharmacology*, 31(9):909–914, 1992.

[8] A. L. Hodgkin and A. F. Huxley. A quantitative description of membrane current and its application to conduction and excitation in nerve. *Journal of Physiology*, 117:500–544, 1952.

[9] M.W. Holladay, M.J. Dart, and J.K. Lynch. Neuronal nicotinic acetylcholine receptors as targets for drug discovery. *Journal of Medicinal Chemistry*, 40(26):4169–4194, 1997.

[10] S.A. Kaiser, L. Soliakov, S.C. Harvey, C.W. Luetje, and S. Wonnacott. Differential inhibition by α-conotoxin-MII of the nicotinic stimulation of [^{3}H]-dopamine release from rat striatal synaptosomes and slices. *Journal of Neurochemistry*, 70(3):1069–1076, 1998.

[11] E.R. Kandel and J.H. Schwartz. *Principles of Neural Science*. Elsevier, 1981.

[12] J.M. Kulak, T.A. Nguyen, B.M. Olivera, and J.M. McIntosh. α-conotoxin MII blocks nicotine-stimulated dopamine release in rat striatal synaptosomes. *Journal of Neuroscience*, 17(14):5263–5270, 1997.

[13] S.Z. Langer. 25 years since the discovery of presynaptic receptors: present knowledge and future perspectives. *Trends in Pharmacological Sciences*, 18:95–99, 1997.

[14] P.M. Lippiello, S.B. Sears, and K.G. Fernandes. Kinetics and mechanism of L-[^{3}H]nicotine binding to putative high affinity receptor sites in rat brain. *Molecular Pharmacology*, 31:392–400, 1987.

[15] N.C.L. McNaughton and A.D. Randall. Electrophysiological properties of the human N-type Ca^{2+} channel. 1. channel gating in Ca^{2+}, Ba^{2+} and Sr^{2+} containing solutions. *Neuropharmacology*, 36(7):895–915, 1997.

[16] I. M. Mintz, B. L. Sabatini, and W. G. Regehr. Calcium control of transmitter release at a cerebellar synapse. *Neuron*, 15:675–688, 1995.

[17] L. Molloy, S. Wonnacott, T Gallagher, P.A. Brough, and B.G. Livett. Anatoxin-a is a potent agonist of the nicotinic acetylcholine receptor of bovine adrenal chromaffin cells. *European Journal of Pharmacology*, 289:447–453, 1995.

[18] P.Whiteaker. *Comparison of the effects of nicotine and isoarecolone on nAChR*. PhD thesis, University of Bath, 1996.

[19] A. Randall and R.W. Tsien. Pharmacological dissection of multiple types of Ca^{2+} channel currents in rat cerebellar granule neurons. *Journal of Neuroscience*, 15(3):2218–2224, 1995.

[20] C. Rapier, G.G. Lunt, and S. Wonnacott. Stereoselective nicotine-induced release of dopamine from striatal synaptosomes: Concentration dependence and repetitive stimulation. *Journal of Neurochemistry*, 50(4), 1988.

[21] C. Rapier, G.G. Lunt, and S. Wonnacott. Nicotinic modulation of [^{3}H]dopamine release from striatal synaptosomes - pharmacological characterisation. *Journal of Neurochemistry*, 54(3):937–945, 1990.

[22] L.W. Role and D.K. Berg. Nicotinic receptors in the development and modulation of CNS synapses. *Neuron*, 16(6):1077–1085, 1996.

[23] P. Sah, A. J. Gibb, and P. W. Gage. The sodium current underlying action potentials in guinea pig hippocampal CA1 neurons. *Journal of General Physiology*, 91:373–398, 1988.

[24] S.M. Simon and R.R. Llinás. Compartmentalization of the submembrane calcium activity during calcium influx and its significance in transmitter release. *Biophysical Journal*, 48:485–498, 1985.

[25] L. Soliakov, T. Gallagher, and S. Wonnacott. Anatoxin-a-evoked [^{3}H]dopamine release from rat striatal synaptosomes. *Neuropharmacology*, 34(11):1535–1541, 1995.

[26] L. Soliakov and S. Wonnacott. Voltage-sensitive Ca^{2+} channels involved in nicotinic receptor-mediated [^{3}H] dopamine release from rat striatal synaptosomes. *Journal of Neurochemistry*, 67(1):163–170, 1996.

[27] R.D. Traub, R.K.S. Wong, R. Miles, and H. Michelson. A model of a CA3 hippocampal pyramidal neuron incorporating voltage-clamp data on intrinsic conductances. *Journal of Neurophysiology*, 66(2):635–650, 1991.

[28] T.J. Turner and K. Dunlap. Pharmacological characterization of presynaptic calcium channels using subsecond biochemical measurements of synaptosomal neurosecretion. *Neuropharmacology*, 34(11):1469–1478, 1995.

[29] M. Umemiya and A.J. Berger. Single channel properties of four calcium channel types in rat motoneurons. *Journal of Neuroscience*, 15(4):2995–3012, 1995.

[30] S. Wonnacott. Presynaptic nicotinic ACh receptors. *Trends in Neurosciences*, 20:92–98, 1997.

A Default Ion Concentrations

Table A.1 contains the normal concentrations of ion species used for the model when the cell is resting. The extracellular concentrations are the same as those used in the normal superfusion buffer and are typical mammalian values (see section 2). Certain superfusion

experiments use a modified buffer which can alter these concentrations, in which case we change the values as follows:
KCl stimulation: Potassium concentration set to the value of the KCl concentration.
Low Na^+ (10mM) buffer: Extracellular sodium set to 10mM.
Calcium free buffer: Extracellular calcium set to 1nM (a small, non-zero value).
The extracellular concentrations are held constant throughout the simulation runs because the superfusion process delivers a constant stream of steady concentration buffer [25],[18].

The intracellular concentrations of potassium and sodium are taken to be typical mammalian ([11]), valid as we would expect a mammalian cell with mammalian extracellular concentrations to have the correct intracellular concentrations. These values are held constant throughout the simulations as the appropriate ion influx causes an insignificant change in their concentration (unpublished results from the model).

	Intra.(mM)	Extra. (mM)
Potassium	120	3.6
Sodium	5	150
Calcium	0.001	2

Table A.1: Default extra- and intracellular ion concentrations for the resting cell.

B Model Equations

All equations are specified for SI units except for transmitter release, which is scaled to return values in counts per minute. Unless otherwise stated, these equations are applied to all terminals.

B.1 Conservation of Current

Kirchoff's conservation of current law for a membrane of potential V_m relative to the cell exterior, electrical capacitance C_m with current influx due to potassium, sodium, nicotinic receptor channels and membrane leakage current (section 2).

$$C_m \frac{dV_m}{dt} + I_K + I_{Na} + I_R + I_{\text{leak}} = 0 \tag{10}$$

$$C_m = 1.57 \times 10^{-12} \tag{11}$$

For terminals that do not possess nAChR, naturally $I_R = 0$.

B.2 Nernst Potentials

For an ion species z with extracellular and intracellular concentrations $[\mathrm{z}]_o$ and $[\mathrm{z}]_i$ respectively we use the Nernst equation [11]:

$$E_z = \frac{25 \times 10^{-3}}{\text{valency}} \ln \left(\frac{[z]_o}{[z]_i} \right). \tag{12}$$

B.3 Delayed Rectifying Potassium Channel

Equations from [23], see section 2.2.2.

$$
\begin{aligned}
I_K &= \bar{g_K} m(E_K - V_m) && (13)\\
\bar{g_K} &= 1.0 \times 10^{-7} && (14)\\
\frac{dm}{dt} &= \alpha_m(V_m)(1-m) - \beta_m(V_m)m && (15)\\
\alpha_m(V_m) &= \frac{16000(V_m + 0.0249)}{1 - \exp\left(-\frac{V_m+0.0249}{0.005}\right)} && (16)\\
\beta_m(V_m) &= 250 \exp\left(-\frac{V_m + 0.04}{0.04}\right) && (17)
\end{aligned}
$$

B.4 Sodium Channel

Equations from [23], see section 2.2.3.

$$
\begin{aligned}
I_{Na} &= \bar{g_{Na}} r^2 s(E_{Na} - V_m) && (18)\\
\bar{g_{Na}} &= 1.0 \times 10^{-9} && (19)\\
\frac{dr}{dt} &= \alpha_r(V_m)(1-r) - \beta_r(V_m)r && (20)\\
\alpha_r(V_m) &= \frac{-3.2 \times 10^5(0.0469 + V_m)}{\exp\left(\frac{V_m+0.0469}{0.004}\right) - 1} && (21)\\
\beta_r(V_m) &= \frac{2.8 \times 10^5(0.0169 + V_m)}{\exp\left(\frac{V_m+0.0199}{0.005}\right) - 1} && (22)\\
\frac{ds}{dt} &= \alpha_s(V_m)(1-s) - \beta_s(V_m)s && (23)\\
\alpha_s(V_m) &= 128 \exp\left(-\frac{V_m + 0.028}{0.018}\right) && (24)\\
\beta_s(V_m) &= \frac{4 \times 10^3}{1 + \exp\left(-\frac{V_m+0.005}{0.005}\right)} && (25)
\end{aligned}
$$

B.5 N-type Calcium Channel

Activation curve x_∞ and inactivation curve y_∞ from [15] with time constant of activation τ_x from [19], time constant of inactivation τ_y chosen to fit with the experimental data, see section 2.2.1.

$$
\begin{aligned}
x_\infty(V_m) &= \frac{1}{1 + \exp(-\frac{V_m+0.0045}{0.0052})} && (26)\\
\tau_x &= 0.001 && (27)\\
y_\infty(V_m) &= \frac{1}{1 + \exp(\frac{V_m+0.074}{0.0065})} && (28)\\
\tau_y &= 0.150 && (29)
\end{aligned}
$$

B.6 P-type Calcium Channel

Activation curve p_∞ from [29] with time constant of activation τ_p from [19], see section 2.2.1.

$$p_\infty(V_m) = \frac{1}{1+\exp(-\frac{V_m+0.0072}{0.0027})} \tag{30}$$

$$\tau_p = 0.0012 \tag{31}$$

B.7 Leakage current

From section 2.2.4.

$$I_{\text{leak}} = \frac{E_m - V_m}{R_m} \tag{32}$$

$$E_m = -0.010 \tag{33}$$

$$R_m = 1.59 \times 10^{12} \tag{34}$$

B.8 Nicotinic Receptor

From section 2.3, current due to nicotinic receptors:

$$I_R = \bar{g_R} X^2 (E_R - V_m) \tag{35}$$

$$E_R = E_{Na} \tag{36}$$

$$\bar{g_R} = 5 \times 10^{-9}. \tag{37}$$

Receptor binding site transition equations, from [14], where [n] is agonist concentration.

$$\frac{dX}{dt} = k_1[\mathrm{n}](1 - X - Y - Z) + k_4 Y - k_2 X - k_3 X \tag{38}$$

$$\frac{dY}{dt} = k_3 X - k_4 Y + k_5[\mathrm{n}]Z - k_6 Y \tag{39}$$

$$\frac{dZ}{dt} = k_7(1 - X - Y - Z) - k_8 Z + k_6 Y - k_5[\mathrm{n}]Z. \tag{40}$$

With the parameters given by:

$$k_1 = 500 \tag{41}$$

$$k_2 = 0.075 \tag{42}$$

$$k_3 = 0.00367 \tag{43}$$

$$k_4 = 0.00005 \tag{44}$$

$$k_5 = 500 \tag{45}$$

$$k_6 = 0.00067 \tag{46}$$

$$k_7 = 0.0001 \tag{47}$$

$$k_8 = 0.00015. \tag{48}$$

B.9 Transmitter Release

B.9.1 Internal Calcium Due to an Open Channel

Where $[\mathrm{Ca}]_\mathrm{o}$ is the extracellular calcium concentration

$$c([\mathrm{Ca}]_\mathrm{o}, V_m) := [\mathrm{Ca}]_\mathrm{o} \exp(-80 V_m). \tag{49}$$

B.9.2 Transmitter Pool

For each type of terminal let ν be the amount of transmitter available in counts per minute (cpm) and $R_\mathrm{term}(t)$ as defined below, then for a constant term of pool replenishment we have:

$$\frac{d\nu}{dt} = \begin{cases} -\frac{d}{dt} R_\mathrm{term}(t) & \text{if } \nu \geq 34000, \\ 570 - \frac{d}{dt} R_\mathrm{term}(t) & \text{otherwise.} \end{cases} \tag{50}$$

B.9.3 Steady-state Release

See section 2.4.3. Expected release for terminals with N-type calcium channels given by given by

$$\frac{dR_\mathrm{Ns}}{dt}(t) = K_N x_\infty(V_m) y_\infty(V_m) c([\mathrm{Ca}]_\mathrm{o}, V_m)^2 \tag{51}$$

and for terminals with P-type calcium channels

$$\frac{dR_\mathrm{Ps}}{dt}(t) = K_P p_\infty(V_m) c([\mathrm{Ca}]_\mathrm{o}, V_m)^4. \tag{52}$$

B.9.4 Release due to Changing Potential

See section 2.4.2. Expected release for terminals with N-type calcium channels given by

$$\frac{dR_\mathrm{Np}}{dt}(t) = \begin{cases} 0 & \text{if } V_m(t-T_N) > \\ & \quad \inf\{V_m(\tau) : t - T_N < \tau < t\}, \\ 65880 \frac{d}{dV} x_\infty(V_m(t-T_N)) c([\mathrm{Ca}]_\mathrm{o}, V_m(t))^2 & \text{otherwise.} \end{cases} \tag{53}$$

$$T_N = 0.7 \tag{54}$$

and for terminals with P-type calcium channels

$$\frac{dR_\mathrm{Pp}}{dt}(t) = \begin{cases} 0 & \text{if } V_m(t-T_P) > \\ & \quad \inf\{V_m(\tau) : t - T_P < \tau < t\}, \\ 7650 \frac{d}{dV} p_\infty(V_m(t-T_P)) c([\mathrm{Ca}]_\mathrm{o}, V_m(t))^4 & \text{otherwise.} \end{cases} \tag{55}$$

$$T_P = 0.8 \tag{56}$$

B.9.5 Combined Release

Unweighted release by a single terminal allowing for transmitter availability

$$\frac{d}{dt}R_{\mathrm{term}}(t) = \begin{cases} \frac{dR_{-\mathrm{s}}}{dt}(t) + \frac{dR_{-\mathrm{p}}}{dt}(t) & \text{if } \nu > 0, \\ 0 & \text{if } \nu = 0. \end{cases} \tag{57}$$

Hence for the total preparation, where $R_{\mathrm{I}}(t)$, $R_{\mathrm{II}}(t)$ and $R_{\mathrm{III}}(t)$ represent the three terminal types,

$$R_{\mathrm{Total}}(t) = 0.5 \times R_{\mathrm{I}}(t) + 0.42 \times R_{\mathrm{II}}(t) + 0.08 \times R_{\mathrm{III}}(t). \tag{58}$$